Magnetic Resonance in Medicine 50:461–467 (2003)

Breathhold Abdominal and Thoracic Proton MR Spectroscopy at 3T

Rachel Katz-Brull, Neil M. Rofsky, and Robert E. Lenkinski*

The clinical utility of proton MR spectroscopy (^{1}H-MRS) has been well demonstrated in the brain, prostate, and breast. The aims of this work were to investigate 1) the feasibility of abdominal and thoracic ^{1}H-MRS at 3T, 2) the benefits of breathholding to MRS in these regions, and 3) the utility of multiple breathhold averaging for MRS. Breathholding either eliminated or markedly reduced phase and frequency shifts and outer voxel contamination that were associated with the motion of the abdomen and the thorax during breathing. Breathholding was found to be essential to spectroscopic investigation of the thorax. Spectra of renal cell carcinoma metastases in the abdomen and thorax were obtained utilizing multiple breathhold averaging. These spectra exhibited a resonance at 3.2 ppm attributed to the trimethylamine moiety of choline metabolites. The results of this study suggest a practical strategy for implementation of ^{1}H-MRS in the body. Magn Reson Med 50: 461–467, 2003. © 2003 Wiley-Liss, Inc.

Key words: breathhold; 3T; body; proton MR spectroscopy

The diagnostic utility of abdominal and thoracic MRI depends on spatial resolution, contrast-to-noise ratio, and the ability to deal with motion artifacts. Respiratory motion degrades images through both temporal blurring and the generation of discrete artifacts (1–4). Several techniques can be used to reduce the artifacts of respiratory motion: respiratory gating, respiratory ordered phase encoding (ROPE) (5), navigator gating (6), and signal averaging. None of these methods entirely eliminates the motion-associated degradation of image quality. Breathhold imaging has proved to be far more satisfactory (7–11), but by implication imposes a patient-dependent time limit on the acquisition. One solution to preserving a breathhold approach when trying to implement high-resolution/low signal-to-noise ratio (SNR) imaging strategies is the use of retrospective averaging of individual breathholds (12).

The effects of motion on MR spectroscopy (MRS) include voxel misregistration, phase and frequency shifts that are caused by movement of the tissue through inhomogeneous B_0 and B_1 fields, and phase dispersion that is caused by motion of the spins during the pulsed gradients used for MRS voxel localization. Also, motion will lead to outer voxel contamination which may or may not be apparent in the spectra. For example, consider the lower pole of the kidney, where motion could inadvertently result in sampling the adjacent retroperitoneal fat. The frame-to-frame frequency and phase modulations (13) due to spatial variability in B_0 and B_1 fields can lead to suboptimal summation of the frames and may result in overall line broadening and reduced signal intensity for the water, lipids, and other resonances. The dispersion of the signal phase due to motion during the application of pulsed gradients is dependent on the amplitude and the duration of the gradient, and on the delay between the actual movement and the application of the gradient (14). Several approaches have been suggested in order to overcome the motion-associated degradation of in vivo MR spectra. To overcome spatial misregistration, navigator gating has been introduced into the MRS sequence (14) and prospective and retrospective gating of the MRS acquisition was investigated (15–17). To overcome the effects of frame-to-frame frequency and phase modulations, phase regularization algorithms have been developed (13). MR sequences with an even number of refocusing pulses given at equal time intervals ("even-echo rephasing" (18)) such as the point-resolved spectroscopy (PRESS) sequence may reduce the susceptibility of MRS to motion. However, these methods did not completely eliminate the effects of spatial misregistration.

The recent installation of higher field strength (3T) clinical magnets with multicoil arrays for the body offer new opportunities for performing body MR spectroscopy. The improved SNR can reduce acquisition times and the higher field strength also provides better separation of resonances. Capitalizing on these attributes, we saw an opportunity to improve body MRS by combining 3T acquisitions using body multicoil arrays with post-processing summation of breathhold data. The central questions of this study were: 1) Is this approach feasible? 2) Is breathholding of benefit to MRS of the abdomen and thorax? and 3) Can multiple breathhold averaging improve the results of abdominal and thoracic MRS?

MATERIALS AND METHODS

This work was performed as part of a larger study aimed at finding surrogate MR markers for response of renal cancer to an antiangiogenic treatment. Patients with renal cancer and metastases were recruited for this study through the Massachusetts General Hospital and Dana-Farber Cancer Institute. Informed consent was obtained in accordance with the guidelines of the institutional review boards of the Massachusetts General Hospital,

Department of Radiology, Beth Israel Deaconess Medical Center, Harvard Medical School, Boston, Massachusetts.

Grant sponsors: Novartis Pharma AG; GE Medical Systems.

*Correspondence to: Robert E. Lenkinski, Ph.D., Director, Center for Advanced Imaging, W/CC-090, Beth Israel Deaconess Medical Center, One Deaconess Road, Boston, MA 02215.
E-mail: rlenkins@caregroup.harvard.edu

Received 16 October 2002; revised 2 May 2003; accepted 2 May 2003.
DOI 10.1002/mrm.10560
Published online in Wiley InterScience (www.interscience.wiley.com).

Dana-Farber Cancer Institute, and Beth Israel Deaconess Medical Center.

The studies were performed using a 3T scanner (Signa LX, General Electric, Waukesha, WI) equipped with a body coil (length 53 cm, diameter 55 cm) for RF transmission and a torso phased array coil (four coils, two anterior and two posterior coils, each a rectangle shape of ~35 cm in the superior–inferior direction and 17 cm in the right–left direction) for receiving (Gore, Newark, DE). The same coil was used for MR imaging and spectroscopy. Breathing instructions were explained to the patients before entering the magnet. The patients entered the magnet in a supine position with their feet first.

Anatomical imaging was carried out at end expiration and included coronal T_2-weighted single shot fast spin echo (SS FSE, 18 sec), axial 3D ultrafast gradient echo (UFGRE 3D, 2 × 23 sec), and axial T_2-weighted SS FSE (17 sec). The localizer image for the MRS voxel was selected from the anatomical images. For breathhold spectroscopy the volunteers were given instructions for two hyperventilation cycles to be followed by a breathhold at end expiration. Single voxel PRESS ^{1}H spectra were acquired with a repetition time of 2 sec, time to echo of 144 msec, spectral width of 5000 Hz, and 512 time points. Spectra during free breathing were acquired for 1–2 min (32 to 64 excitations, respectively) with two "dummy" scans. MRS during breathhold was performed in 20 sec. This time frame allowed for two "dummy" scans and eight acquisitions. Each free breathing/breathhold scan was stored as a separate file. Each file included four datasets from the four receiver coils in the torso phased array. The dataset with the best SNR was selected for further analysis. Free induction decays were processed with a line broadening of 7–15 Hz, zero-filled twice, Fourier-transformed, and phase-corrected. Phase correction was performed globally (the same phase correction factor for all frames) or individually for frame-to-frame phase correction, as described in the Results section. After frame-to-frame individual phase correction the frequency of the spectra was registered using the residual water signal at 4.7 ppm. Data processing was performed using SAGE the spectral analysis software provided by General Electric.

RESULTS

The advantages of the breathholding approach are demonstrated in a spectroscopic examination of the lower pole of the kidney. Figure 1a demonstrates the localizer image that was used for selection of the MRS voxel (solid white line). Figure 1b,c demonstrates the frame-to-frame residual water signals in eight scans that were recorded in free breathing and in a breathhold, respectively. The spectra were processed with a global phase correction, preserving relative frame-to-frame phase or frequency variations. The reproducibility of the breathhold spectra is much greater than that of the free-breathing spectra. The sum of the individual frames (in Fig. 1b,c) is shown in Fig. 1d,e, respectively. In the summed spectrum of the breathhold, the water signal intensity is higher compared to free breathing.

The frame-to-frame variations in phase and frequency were corrected in postprocessing with an individual phase correction algorithm and frequency registration of the residual water-signal (see Materials and Methods). The effects of these correction algorithms on the frame-to-frame water signal in the free-breathing and in the breathhold acquisitions are shown in Fig. 1f,g, respectively. The sum of these corrected individual frames is shown in Fig. 1h,i, respectively. Using the correction algorithms the sum of the water signal was similar in free breathing and breathhold.

As a result of the application of these correction algorithms, the frame-to-frame phase and frequency of the lipid signal appeared constant, similar to what was observed in the water signal. However, the frame-to-frame intensity of the lipid signal was highly variable during free breathing (Fig. 2a). In contrast, the frame-to-frame intensity of the lipid signal was reproducible in breathholds (Fig. 2b,c). The sum of these lipid signals in free breathing compared to breathholding is shown in Fig. 2d,e, respectively. These spectra demonstrate higher lipid signal in free breathing. These results suggest that inadvertent sampling of tissue beyond the region of interest (ROI; the latter prescribed on an end-expiration breathhold image) lead to contamination of the spectra by an additional amount of lipids. Note that the retroperitoneal fat is located about 1–2 mm from the edge of the ROI (Fig. 1a). Since breathing may lead to anatomical displacement of up to 2 cm in the superior–inferior direction of the abdomen, it is possible that during free breathing the spectra are sampled from multiple locations in the kidney and its surroundings, including retroperitoneal fat.

The utility of the multiple breathhold summation approach in the investigation of abdominal and thoracic tumors is demonstrated in the next two examples. The first example is of a renal cell carcinoma metastasis in the adrenal gland. The location of the tumor is demonstrated in Fig. 3a and the location of the MRS voxel within the tumor is demonstrated by the outlined area. The spectrum obtained in a single breathhold and the sum of four and eight breathholds at this location are shown in Fig. 3b–d. The large signal at 4.7 ppm is due to residual (partially suppressed) water. The signal at 3.2 ppm was assigned to the trimethylamine moiety (TMA) that is common to the choline-containing compounds. The signal at ~1.3 ppm was assigned to the methyl moieties of fatty acids (lipids). Each breathhold was composed of eight scans (total scan time for eight breathholds was 2.1 min). Individual breathhold data were summed in postprocessing. The SNR of the TMA and lipid signals has increased with the increase in the number of frames (acquired in consecutive breathholds).

The second example is of a thoracic tumor, a metastasis of renal cell carcinoma located in the mediastinum. The tumor and the location of the MRS voxel are demonstrated in Fig. 4a. The proton spectra at this location recorded during free breathing and in breathholds are shown in Fig. 4b,c, respectively. Altogether, 32 frames were recorded in each of these spectra (total scan time was 1.07 min). Breathhold data were summed in postprocessing. As in the

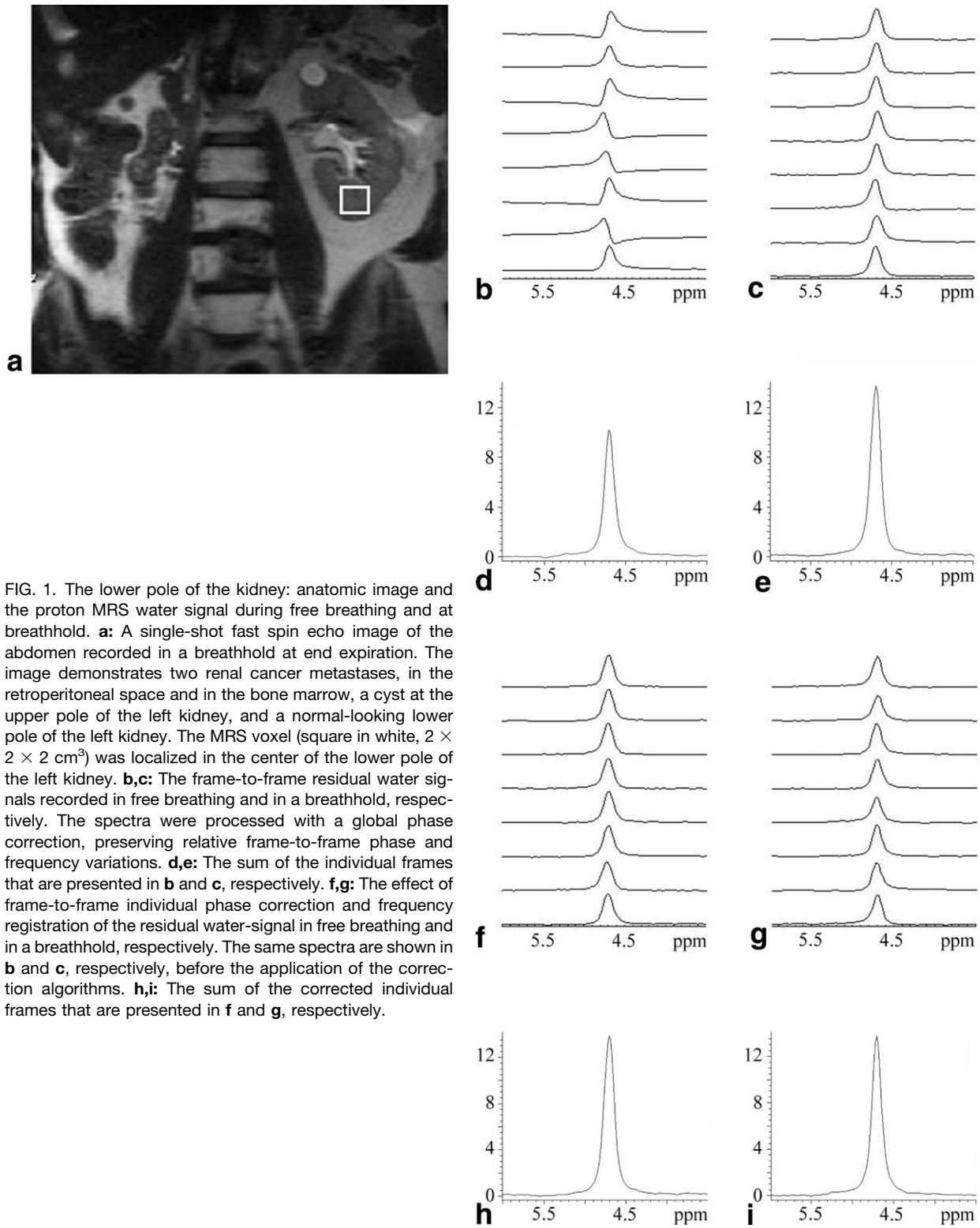

FIG. 1. The lower pole of the kidney: anatomic image and the proton MRS water signal during free breathing and at breathhold. **a:** A single-shot fast spin echo image of the abdomen recorded in a breathhold at end expiration. The image demonstrates two renal cancer metastases, in the retroperitoneal space and in the bone marrow, a cyst at the upper pole of the left kidney, and a normal-looking lower pole of the left kidney. The MRS voxel (square in white, $2 \times 2 \times 2$ cm^3) was localized in the center of the lower pole of the left kidney. **b,c:** The frame-to-frame residual water signals recorded in free breathing and in a breathhold, respectively. The spectra were processed with a global phase correction, preserving relative frame-to-frame phase and frequency variations. **d,e:** The sum of the individual frames that are presented in **b** and **c**, respectively. **f,g:** The effect of frame-to-frame individual phase correction and frequency registration of the residual water-signal in free breathing and in a breathhold, respectively. The same spectra are shown in **b** and **c**, respectively, before the application of the correction algorithms. **h,i:** The sum of the corrected individual frames that are presented in **f** and **g**, respectively.

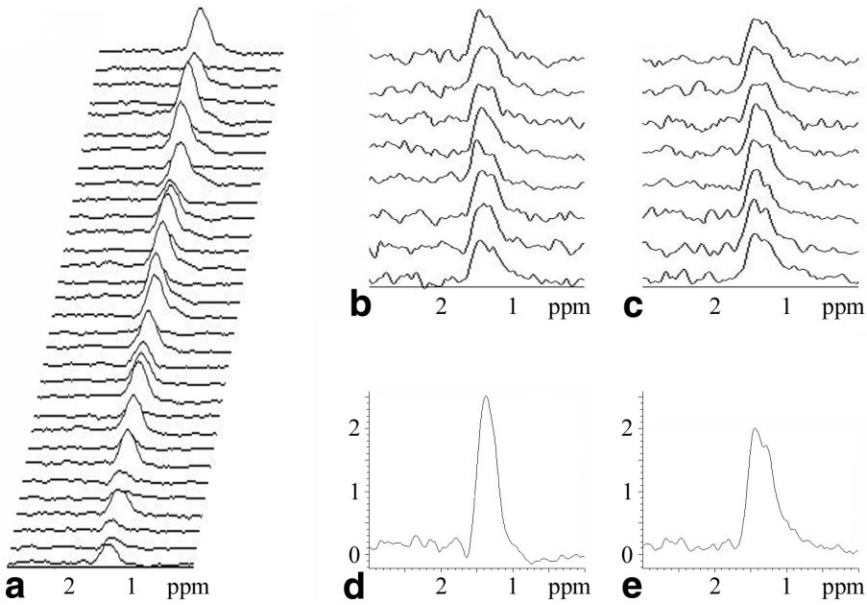

FIG. 2. The lower pole of the kidney: the proton MRS lipid signal during free breathing and at breathhold. The location of the MRS voxel is shown in Fig. 1a. **a:** Frame-to-frame lipid signal during free breathing. The spectra were processed with frame-to-frame individual phase correction and frequency registration as described in Fig. 1; 32 scans are shown, the spectral region of the water signal of the first eight of these scans is presented in Fig. 1f. **b,c:** Frame-to-frame lipid signal in two consecutive breathholds. **d,e:** The lipid signal of the sum of eight scans acquired during free breathing and at a breathhold, respectively. Note the higher lipid signal in free breathing.

adrenal gland metastasis, these spectra are composed of three major components: residual water, TMA, and lipids. The multiple breathhold spectrum shows better SNR for the lipids and the TMA signals.

DISCUSSION

Three factors were combined in this study to enable proton MRS of the abdomen and thorax: high magnetic field, torso multicoil array, and breathholding. In loading samples, the

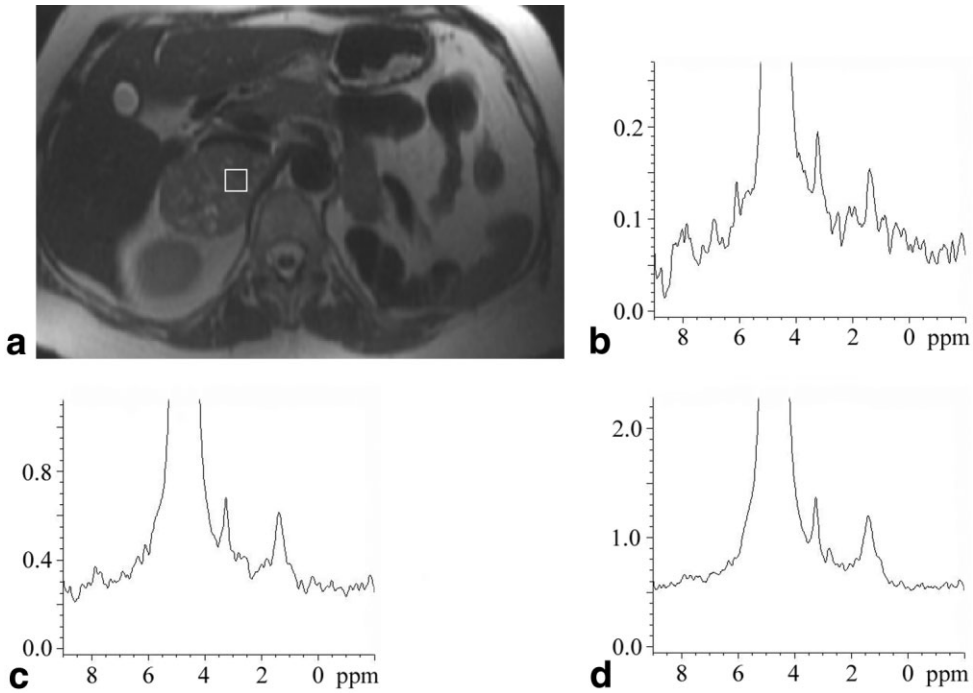

FIG. 3. **a:** A single-shot fast spin echo image of the abdomen recorded in a breathhold at end expiration. A large renal cell carcinoma metastasis in the right adrenal gland is demonstrated. The MRS voxel (square in white, $2 \times 2 \times 2$ cm^3) was localized in the center of the tumor. **b,c,d:** The proton spectrum at the location demonstrated in **a** acquired with one, four, and eight breathholds, (8, 32, and 64 frames, respectively). The total scan time for eight breathholds was 2.1 min. The large signal at 4.7 ppm is due to partially suppressed water. The signal at 3.2 ppm was assigned to the trimethylamine moiety (TMA) that is common to the choline-containing compounds. The linewidth of the TMA signal in this example was 15 Hz. The signal at ~1.3 ppm was assigned to lipids. Breathhold data were summed in postprocessing. Note the improvement in the SNR with the increase in the number of frames.

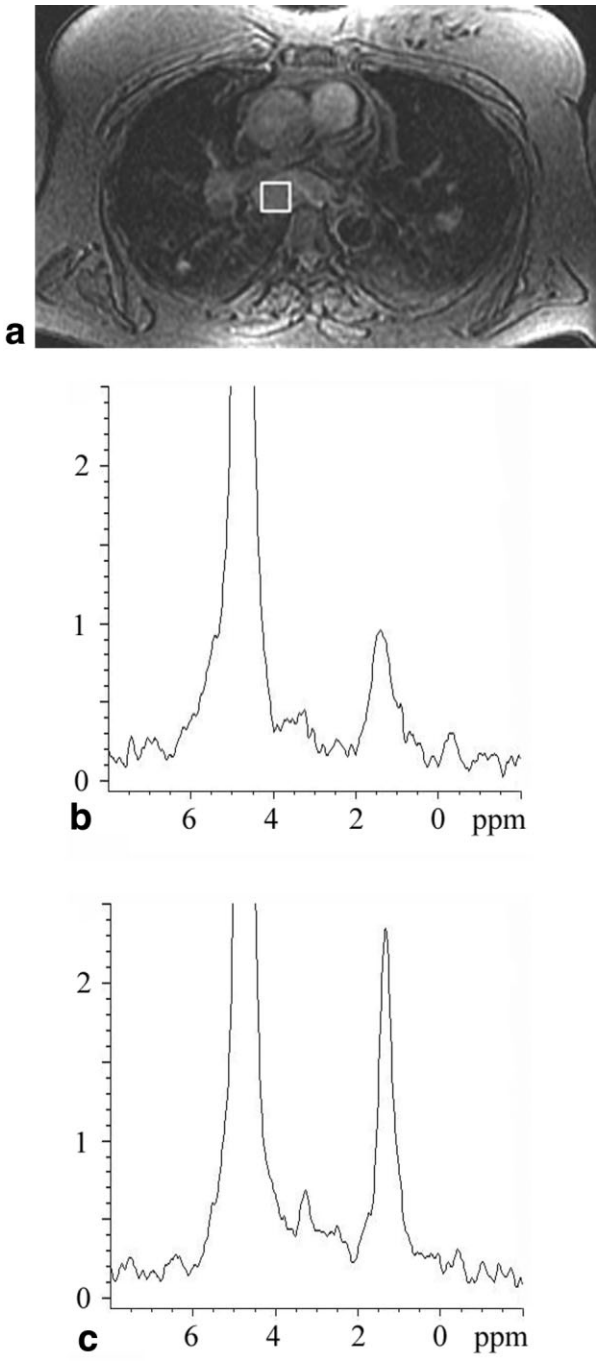

FIG. 4. **a:** A fast gradient echo image of the thorax recorded in a breathhold at end expiration. A large renal cell carcinoma metastasis in the mediastinum is demonstrated. The MRS voxel (outlined area, $2 \times 2 \times 2$ cm^3) was localized in the center of the tumor. **b,c:** The proton spectra at the location demonstrated in **a** acquired during free breathing and in four breathholds, respectively. A total of 32 scans were recorded for each spectrum (1.07 min). Breathhold data were summed in postprocessing. The large signal at 4.7 ppm is due to partially suppressed water. The signal at 3.2 ppm (arrow) was assigned to the trimethylamine moiety (TMA) that is common to the choline-containing compounds. The linewidth of the TMA signal in this example was 25 Hz. The signal at ~1.3 ppm was assigned to lipids. Note the improvement in the SNR of both the TMA and the lipid signals in multiple breathholds compared to free breathing.

SNR varies linearly with field strength (19). Most clinical scanners operate at 1.5T, while the studies described here were performed at 3T. This 2-fold increase in field strength may lead to a 2-fold increase in the SNR in clinical studies. The increase in SNR can be used to reduce scan time by a factor of four. Torso multicoil arrays have gained wide acceptance in abdominal and thoracic imaging at 1.5T. The use of a multicoil array increases the SNR by maximizing the proximity of one of the receiver coils to the ROI. Several studies have demonstrated the SNR advantages of multicoil arrays in MRS examinations (20). The availability of a body coil for the 3T whole body scanner provided the opportunity to implement this approach at this field.

Breathholding contributed to our ability to perform proton MRS in the abdomen and thorax in several ways. First, it either eliminated or significantly reduced frame-to-frame phase and frequency variations, depending on the patients ability to hold their breath. Our initial experience with the breathholding approach shows that some locations in the abdomen were less susceptible than others to frame-to-frame frequency and phase variations. The degree of this susceptibility may be dependent on the location and on the type of breathing that the patient performs (for example, deep or shallow breathing). The multiple breathhold summation improved the quality of most of the spectra, but with varying impact across cases. Nevertheless, the quality of the abdominal breathhold examination was always equal to or better than that of free breathing. In contrast, breathholding was essential in the thorax examinations and always led to a substantial improvement in the SNR and the resolution of signals.

The shortcoming of the breathhold approach is that it may not be well tolerated by all patients. In this study we used eight consecutive breathholds with a 20-sec period of breathholding in each, which was well tolerated by most patients. The first 4 sec of the breathhold were used for two "dummy" scans and 16 sec were used for acquisition of eight scans. The two "dummy" scans were sufficient in all cases to reach a steady state of the magnetization in the ROI. In one case with compromised breathholding ability, we eliminated the "dummy" scans part and acquired the spectra for 16 sec. In this case the first frame showed higher signal than the rest of the frames, which in turn appeared at steady state. The results of the current study suggest that it would be possible to divide the 20-sec breathhold to even shorter periods that may be better tolerated by some patients and sum these breathhold acquisitions retrospectively.

Retrospective summation allows increased acquisition times without introducing motion artifacts. This approach has been successfully applied to body MR imaging (12) and requires reliable image coregistration. In a majority of patients, retrospective image averaging with simple instructions at end-expiration improved SNR without appreciable degradation of spatial resolution (12). Breathhold organ position may be variable in some patients. However, automated techniques that place slices in a fixed position relative to anatomical

landmarks are being developed and should improve coregistration in even recalcitrant cases. Obviously, the patients' ability to perform a breathhold must be considered when implementing or modifying an imaging/spectroscopy protocol for a particular patient. The multiple breathhold exam requires increased communication between the patient and system operator, which may not be possible in all clinical cases. In the current study breathing instructions were discussed with the patient before putting them into the magnet. Exclusion of misregistered datasets from the summation process was sometimes necessary. Further evaluation and optimization in clinical studies will determine the frequency of this data exclusion.

We have confirmed here that frame-to-frame phase correction and frequency registration, using the residual water signal, improved the SNR of the abdominal spectra. This approach has been previously demonstrated using phase regularization algorithm of the residual water (13). However, we have shown that only breathholding can eliminate the contamination of the ROI by signals that originate outside of the ROI. The previous use of navigator gating for displacement registration has resulted in lesser contamination of the data by the use of displacement acceptance criteria (14). However, only a small part of the acquisitions were in general accepted at the locations of full exhalation. Unlike navigator correction for MR imaging methods, the spectra could not be corrected for motion, only accepted or rejected from the sum (14). Breathholding appears to be more time-efficient than navigator echo acquisitions with respect to acquiring the signal from one location at full exhalation.

The breathholding approach might have future utility in multivoxel spectroscopy such as chemical shift imaging (CSI). CSI acquisitions are inherently longer than a breathholding duration. The addition of parallel imaging strategies (21) and/or a segmented acquisition approach may enable the combination of CSI within the time frame of a breathhold. As an example of the impact of using a segmented acquisition, consider an 8×8 CSI matrix that can be obtained within eight breathholds: In each 16-sec breathhold, we can acquire eight phase-encoding steps, each with a repetition time of 2 sec. In eight breathholds, 64 phase-encoding steps can be acquired. By retrospectively combining these phase-encoding steps into one 2D dataset, the cumulative advantages of CSI (multivoxel sampling and averaging over the whole FOV) are obtained. The breathholding segmented CSI approach may lead to a significant improvement in the quality of abdominal CSI data which suffer inherently from large contaminating signals from the surrounding tissue. The contamination of breast CSI spectra due to breathing motion was described in detail in an article by Doyle et al. (22). In this article, it was shown that the CSI voxel contamination effects induced by breathing motion exceeds by far the effects of the point spread function. Specifically, signals that originate in the chest wall propagate throughout *k*-space and therefore contaminate voxels in the breast tissue and significantly alter the metabolite concentration in these voxels of interest. The breathhold approach might be a useful solution to this problem.

In summary, by combining high field strength and localized multicoil array for abdominal and thoracic proton MRS, cumulative improvements in SNR were achieved while breathholding minimized inadvertent sampling of tissues outside the ROI and phase and frequency variations.

ACKNOWLEDGMENTS

We thank David Alsop, Ph.D., Cedric Debazelaire M.D., and Jingbo Zhang, M.D. from the Radiology Department at the Beth Israel Deaconess Medical Center, Daniel George, M.D. from the Dana-Farber Cancer Institute, Dror Michaelson, M.D., Ph.D. from the Massachusetts General Hospital, Napapon Sailasuta, Ph.D. and Thomas Raidy, Ph.D. from GE Medical systems, and Neil Williams, Ph.D. from Gore Inc. for their assistance in the course of this study.

REFERENCES

1. Barish MA, Jara H. Motion artifact control in body MR imaging. Magn Reson Imag Clin N Am 1999;7:289–301.
2. Foo TK, King KF. A computationally efficient method for tracking reference position displacements for motion compensation in magnetic resonance imaging. Magn Reson Med 1999;42:548–553.
3. Gierada DS, Curtin JJ, Erickson SG, Prost RW, Strandtt JA, Goodman LR. Diaphragmatic motion: fast gradient-recalled-echo MR imaging in healthy subjects. Radiology 1995;194:879–884.
4. Mirowitz SA, Lee JK, Brown JJ, Eilenberg SS, Heiken JP, Perman WH. Rapid acquisition spin-echo (RASE) MR imaging: a new technique for reduction of artifacts and acquisition time. Radiology 1990;175:131–135.
5. Bailes DR, Gilderdale DJ, Bydder GM, Collins AG, Firmin DN. Respiratory ordered phase encoding (ROPE): a method of reducing respiratory motion artefacts in MR imaging. J Comput Assist Tomogr 1985;9:835–838.
6. McConnell MV, Khasgiwala VC, Savord BJ, Chen MH, Chuang ML, Edelman RR, Manning WJ. Comparison of respiratory suppression methods and navigator locations for MR coronary angiography. AJR Am J Roentgenol 1997;168:1369–1375.
7. Earls JP, Rofsky NM, DeCorato DR, Krinsky GA, Weinreb JC. Echo-train STIR MRI of the liver: comparison of breath-hold and non-breath-hold imaging strategies. J Magn Reson Imag 1999;9:87–92.
8. Edelman RR, Wallner B, Singer A, Atkinson DJ, Saini S. Segmented turboFLASH: method for breath-hold MR imaging of the liver with flexible contrast. Radiology 1990;177:515–521.
9. Gaa J, Hatabu H, Jenkins RJ, Finn JP, Edelman RR. Replacement of conventional T2-weighted imaging with breath-hold MR imaging. Radiology 1996;200:459–464.
10. Rofsky NM, Lee VS, Laub G, Pollack MA, Krinsky GA, Thomasson D, Ambrosino MM, Weinreb JC. Abdominal MR imaging with a volumetric interpolated breath-hold examination. Radiology 1999;212:876–884.
11. Marks B, Mitchell DG, Simelaro JP. Breath-holding in healthy and pulmonary-compromised populations: effects of hyperventilation and oxygen inspiration. J Magn Reson Imag 1997;7:595–597.
12. Feinberg DA, Rofsky NM, Johnson G. Multiple breath hold average (MBA) method for increased SNR in rapid abdominal MRI. Magn Reson Med 1995;34:905–909.
13. Star-Lack JM, Adalsteinsson E, Gold GE, Ikeda DM, Spielman DM. Motion correction and lipid suppression for ^{1}H magnetic resonance spectroscopy. Magn Reson Med 2000;43:325–330.
14. Tyszka JM, Silverman JM. Navigated single-voxel proton spectroscopy of the human liver. Magn Reson Med 1998;39:1–5.

15. Pattany PM, Khamis IH, Bowen BC, Goodkin K, Weaver RG, Murdoch JB, Donovon Post MJ, Quencer RM. Effects of physiologic human brain motion on proton spectroscopy: quantitative analysis and correction with cardiac gating. Am J Neuroradiol 2002;23:225–230.
16. Felblinger J, Jung B, Slotboom J, Boesch C, Kreis R. Methods and reproducibility of cardiac/respiratory double-triggered (^{1})H-MR spectroscopy of the human heart. Magn Reson Med 1999;42:903–910.
17. Felblinger J, Kreis R, Boesch C. Effects of physiologic motion of the human brain upon quantitative ^{1}H-MRS: analysis and correction by retro-gating. NMR Biomed 1998;11:107–114.
18. Waluch V, Bradley WG. NMR even echo rephasing in slow laminar-flow. J Comput Assist Tomogr 1984;8:594–598.
19. Haacke EM, Brown RW, Thompson MR, Venkatesan R. Magnetic resonance imaging physical principles and sequence design. New York: John Wiley & Sons; 1999.
20. Nelson SJ, Vigneron DB, Star-Lack J, Kurhanewicz J. High spatial resolution and speed in MRSI. NMR Biomed 1997;10:411–422.
21. Sodickson DK, McKenzie CA. A generalized approach to parallel magnetic resonance imaging. Med Phys 2001;28:1629–1643.
22. Doyle VL, Howet FA, Griffiths JR. The effect of respiratory motion on CSI localized MRS. Cooperative Group on MR Applications to Cancer. Phys Med Biol 2000;45:2093–2104.